Academic Journal of Computing & Information Science
ISSN 2616-5775 Vol. 6, Issue 11: 151-158, DOI: 10.25236/AJCIS.2023.061119

Optimization Design Study of Heliostat Field Based on Particle Swarm Algorithm

Kaiduo Wen[1, *]

[1]*Emergency Management College, Nanjing University of Information Science and Technology, Nanjing, China*
[*]*Corresponding author: 202183360046@nuist.edu.cn*

Abstract: *This paper focuses on the in-depth study of the layout of the heliostat and absorption tower in tower solar thermal power generation. Preliminary optical efficiency calculations are carried out using the solar position model and the reflected light model. Firstly, the solar azimuth angle and solar altitude angle at a specific moment are clarified. Secondly, the reflection of solar rays in the mirror field and its interaction with the absorber tower are simulated. Finally, the layout of heliostat mirrors is optimized by the particle swarm algorithm, and the key layout parameters are obtained.*

Keywords: *Tower Solar, Heliostat Layout, Optical Efficiency, Particle Swarm Algorithm, Light Simulation*

1. Introduction

Energy is closely linked to human economic activities and productive life, and the world is currently facing a severe energy situation. Promoting energy technology innovation and its structural transformation is the common pursuit of the world today. Solar energy, as a rich renewable resource, has been rapidly developing its power generation technology, among which the optimized design of tower-type solar thermal power plant and its heliostat field is particularly critical [1, 2]. In view of this, this paper plans to study a circular heliostat mirror field in a specific area, mainly to solve two major problems: 1) to determine the annual average optical efficiency and thermal power output of the absorber tower at the center of the heliostat mirror field, and 2) to design the optimal parameters of the heliostat mirror field under the condition of ensuring that the field reaches the rated power to ensure that the annual average thermal power output per unit of the mirror surface area is maximized.

2. The heliostat field model

2.1 Solar Position Model

The concept of celestial sphere in astronomy, which is defined as a sphere coinciding with the center of the Earth, having the same rotation axis, and having an infinite radius, is used in this paper for an in-depth study [3]. The time-angle coordinate system is a celestial sphere coordinate system that utilizes the time angle and the declination angle to determine the position of the target celestial body. The hour angle is the angle between the plane of the meridian circle and the plane of the meridian circle through which the projection point of the target object position on the celestial sphere passes. And the declination angle is the angle between the line connecting the position of the celestial body with the earth's center and the equatorial plane. In this coordinate system, the solar time angle and solar declination angle of the sun to the earth are defined. The geocentric coordinate system, on the other hand, takes the target position as the coordinate origin and the horizon at that position as the reference plane, and its spatial right-angle coordinate system is defined as due east as the positive direction of the X-axis, due north as the positive direction of the Y-axis, and zenith as the positive direction of the Z-axis. In this coordinate system, the angle between the line connecting the sun and the coordinate origin and the ground plane, as well as the angle between the projection of the line connecting the sun and the coordinate origin on the datum plane and the positive direction of the Y-axis are defined, as shown in Figures 1 and 2.

ISSN 2616-5775 Vol. 6, Issue 11: 151-158, DOI: 10.25236/AJCIS.2023.061119

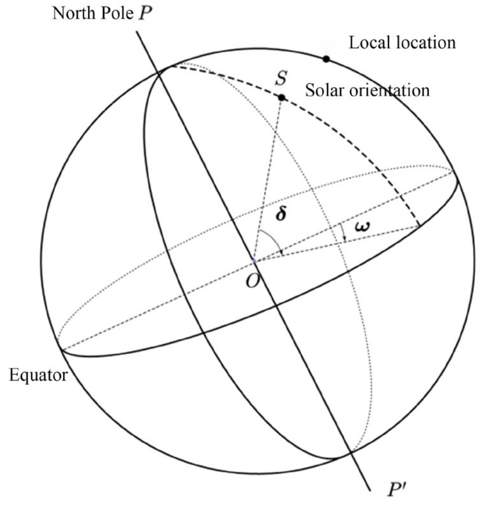

Figure 1: Time-angle coordinate system

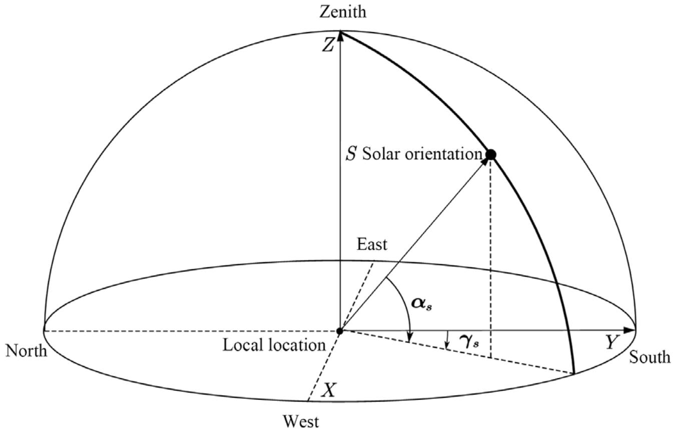

Figure 2: Horizontal coordinate system

1) Calculation of solar time angle ω

The solar time angle represents the angle of rotation of the earth per unit of time, so the calculation of the time angle is related to time. In this paper, a certain time is noted as ST, and the formula for the calculation of ω is given as follows:

$$\omega = \frac{\pi}{12}(ST - 12) \tag{1}$$

2) Calculation of solar declination angle δ

The angle of solar declination is the angle formed between the earth-sun line and the earth's equatorial plane and is related to the tilt of the earth's axis and the earth's rotation. In this paper, the vernal equinox (March 21) is taken as day 0 for day notation, and D is recorded as the date of the day. For example, April 1 corresponds to D=11. Accordingly, the formula for δ is as follows:

$$\sin\delta = \sin\frac{2\pi D}{365}\sin(\frac{2\pi}{360}23.45) \tag{2}$$

3) Calculation of solar altitude angle α_s

The horizon coordinate system in this paper coincides with the mirror field coordinate system, and the target location is the center of the circular heliostat mirror field (located at 98.5°E, 39.4°N). Noting the local latitude as δ, α_s is calculated as follows:

$$\sin\alpha_s = \cos\delta\cos\varphi\cos\omega + \sin\delta\sin\varphi \tag{3}$$

ISSN 2616-5775 Vol. 6, Issue 11: 151-158, DOI: 10.25236/AJCIS.2023.061119

4) Calculation of solar azimuth α_s

Knowing ω, δ, α_s the solar azimuth γ_s can be calculated according to the following equation.

$$\cos\gamma_s = \frac{\sin\delta - \sin\alpha_s \sin\varphi}{\cos\alpha_s \cos\varphi} \tag{4}$$

The solar position parameters ω, δ, α_s and γ_s.

2.2 Reflected light model

(1) Calculation of the distance d_{HR} between the center of the mirror and the center of the collector and the angle τ

According to the collinearity theorem, the solution formula for d_{HR} is as follows:

$$d_{HR} = \sqrt{x^2 + y^2 + (h_T - h)^2} \tag{5}$$

Therefore, it can be obtained:

$$\tan\tau = \frac{80 - h}{\sqrt{x^2 + y^2}} \tag{6}$$

(2) Calculation of the angle between the normal direction of the heliostat and the incident light θ and the pitch angle σ

As shown in Figure. 3, based on the analysis of the geometrical relationship between the incident light in the normal plane of the fixed heliograph, the following equational relationship can be derived:

$$\sin\alpha_s = \sin(2\theta + \tau) \tag{7}$$

$$\cos\sigma = \cos\left(\frac{\pi}{2} - \theta - \tau\right) = \sin(\theta + \tau) \tag{8}$$

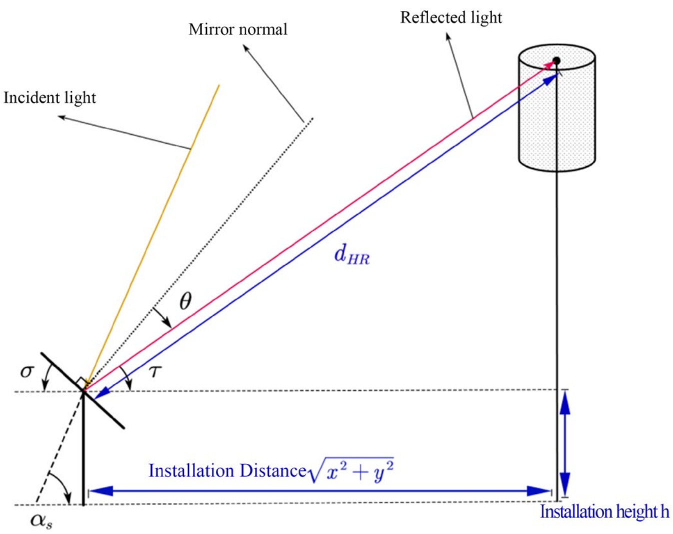

Figure 3: Schematic of the geometric relationship between the angles within the heliostat

2.2 Optical efficiency model

The optical efficiency of a fixed-sun mirror field is defined as the ratio of the energy ultimately received by the collector to the total energy of the incident light. At any given moment, the optical efficiency can be solved based on the following equation.

$$\eta = \eta_{cos}\eta_{sb}\eta_{at}\eta_{trunc}\eta_{ref} \tag{9}$$

Where η_{cos} refers to cosine efficiency, η_{sb} refers to shadow shading efficiency, η_{at} refers to

ISSN 2616-5775 Vol. 6, Issue 11: 151-158, DOI: 10.25236/AJCIS.2023.061119

atmospheric transmittance, η_{trunc} refers to collector truncation efficiency, and η_{ref} refers to specular reflectance.

The cosine value of the angle between the normal direction of the heliostat and the incident light θ, i.e., the cosine efficiency. According to Eq. (6-7) can be solved for θ, therefore:

$$\eta_{cos} = cos\,\theta \tag{10}$$

Remember that the total number of incident rays of the fixed eyepiece in the absence of shading is n_{all}, the number of incident shading rays is n_{IL}, and the number of reflected shading rays is n_{RL}. Remember that the shadow area produced by the tower projection is S_T and the total footprint of the heliostat field is S. Therefore, the following formula for η_{sb} is proposed:

$$\eta_{sb} = 1 - \frac{n_{IL}+n_{RL}}{n_{all}} - \frac{S_T}{S} \tag{11}$$

In conjunction with the above, the normal vectors of the mirror can be further found by following the specular coordinate system established by the question, which gives the incident and reflected rays at any point on the fixed-heaven mirror. By establishing the specular coordinate system, obtain the coordinates of any point on the mirror. Convert the mirror surface coordinates to the mirror field coordinates to establish the coordinate equations of the incident and reflect light lines and the mirror surface. And by calculating the intersection situation between the mirrors, n_{IL} and n_{RL} can be derived.

Calculating the η_{sb_i} of the ith heliostat, it is known to memorize the equation of the incident light of the ith heliostat as: $\frac{x_i-x_{R_i}}{in_i(x)} = \frac{y_i-y_{R_i}}{in_i(y)} = \frac{z_i-z_{R_i}}{in_i(z)}$,The equation of the reflected ray is: $\frac{x_i-x_{R_i}}{re_i(x)} = \frac{y_i-y_{R_i}}{re_i(y)} = \frac{z_i-z_{R_i}}{re_i(z)}$. Assume that the mirror equation for the n(n≠i) fixed-sun mirror is: $x_{nor_n}(x_n - x_{C_n}) + y_{nor_n}(y_n - y_{C_n}) + z_{nor_n}(z_n - z_{C_n}) = 0$. By combining the above three equations, the intersection of incident blocking rays and the intersection of reflected blocking rays on the ith heliostat can be found separately. Calculating the number of all intersection points gives n_{RL} and n_{IL}. The scenario simulation is shown in Figure 4.

Using α_s, the direction of incidence of sunlight can be determined, and by multiplying the product of $\cos\alpha_s$ and the cross-sectional area of the tower, the area of shadow formed by the tower, S_T, can be determined. The scenario simulation is shown in Figure 5.

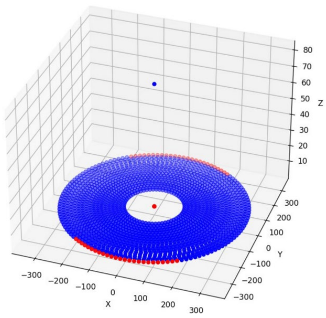

Figure 4: Simulation of inter-sunset mirror shading

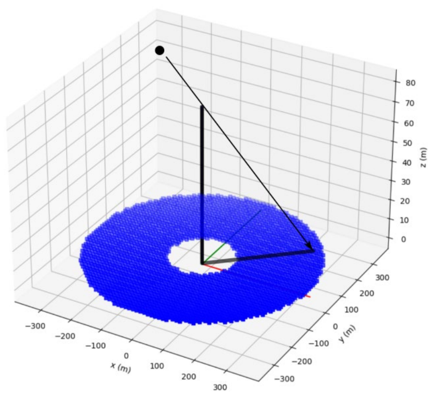

Figure 5: Simulation of tower projection

ISSN 2616-5775 Vol. 6, Issue 11: 151-158, DOI: 10.25236/AJCIS.2023.061119

Sunlight loses energy during reflection due to obstruction by impurity particles in the air. The value of atmospheric transmittance η_{at} is related to the reflectance distance d_{HR} and is calculated by the following formula:

$$\eta_{at} = 0.99321 - 0.0001176 d_{HR} + 1.97 \times 10^{-8} \times {d_{HR}}^2 (d_{HR} \leq 1000) \tag{12}$$

Define the truncation efficiency of the collector η_{trunc} as the ratio of the number of reflected rays received by the collector, n_T, to the number of rays effectively reflected by the heliostat. The calculation formula is as follows:

$$\eta_{trunc} = \frac{n_T}{n_{all} - (n_{IL} + n_{RL})} \tag{13}$$

Based on the literature, this paper solves for η with a constant value of η_{sb}=0.9400.

The specular reflectivity η_{ref} can be taken as a constant, and in this paper, it is taken as 0.92. According to the output thermal power calculation formula for a fixed-sun mirror field:

$$E_{field} = DNI \cdot \sum_i^N A_i \eta_i \tag{14}$$

Where DNI denotes the normal direct radiation irradiance, which refers to the solar radiation energy per unit time taken over by the average unit area of the earth perpendicular to the line of elevation of the eye. n denotes the total number of heliostats in the heliostat field. A_i denotes the area of the ith heliostat, and η_i denotes the optical efficiency of the ith heliostat. A_i can be derived from the dimensions of the heliostat, based on which each heliostat's η_i can be solved for. DNI can be solved by the following equation:

$$\begin{cases} DNI = G_0 \left[a + b \cdot exp(-\frac{c}{\sin \alpha_s}) \right] \\ a = 0.4237 - 0.00821(6 - H)^2 \\ b = 0.5055 - 0.00595(6.5 - H)^2 \\ c = 0.2711 - 0.01858(2.5 - H)^2 \end{cases} \tag{15}$$

Where G_0 is the solar constant, whose value is taken as 1.366 kW/m^2 and H is the altitude.

Noting that the average thermal power output per unit area of mirror is $E_{\overline{field}}$, and the average annual thermal power output is $\overline{E_{field}}$, then:

$$E_{\overline{field}} = \frac{E_{field}}{\sum_i^N A_i} = \frac{DNI \cdot \sum_i^N A_i \eta_i}{\sum_i^N A_i} \tag{16}$$

$$\overline{E_{field}} = \frac{\sum_{k=1}^{12} (E_{field})_k}{12} = \frac{\sum_{k=1}^{12} (DNI \cdot \sum_i^N A_i \eta_i)_k}{12} \tag{17}$$

where k denotes the month, k = 1, ..., 12. Record the average annual thermal power output E per unit area of mirror, then:

$$E = \frac{\overline{E_{field}}}{\sum_i^N A_i} = \frac{\sum_{k=1}^{12} (DNI \cdot \sum_i^N A_i \eta_i)_k}{12 \sum_i^N A_i} \tag{18}$$

In this paper, the 21st day of each month can be used as an example to determine the positional parameters of the sun. Obtain the coordinate information of each heliostat on the site. Combined with the geographic location, heliostat size and absorption tower size data, the results of the calculation of the relevant indicators are shown in Tables 1 and 2:

ISSN 2616-5775 Vol. 6, Issue 11: 151-158, DOI: 10.25236/AJCIS.2023.061119

Table 1: Average optical efficiency and power output on the 21st day of each month

Data	Average optical efficiency	Average cosine efficiency	Average shadow masking efficiency	Average truncation efficiency	Average annual power output per unit area (kW/m^2)
January 21	0.7558	0.9298	0.9739	0.9400	0.6567
February 21st	0.7366	0.9012	0.9791	0.9400	0.6937
March 21st	0.7080	0.8631	0.9828	0.9400	0.7037
April 21st	0.6703	0.8182	0.9816	0.9400	0.6890
May 21st	0.6481	0.7828	0.9919	0.9400	0.6767
June 21st	0.6340	0.7690	0.9878	0.9400	0.6650
July 21st	0.6390	0.7816	0.9795	0.9400	0.6674
August 21st	0.6755	0.8175	0.9900	0.9400	0.6946
September 21st	0.7150	0.8638	0.9917	0.9400	0.7102
October 21st	0.7375	0.9042	0.9773	0.9400	0.6905
November 21st	0.7722	0.9301	0.9947	0.9400	0.6701
December 21st	0.7801	0.9400	0.9943	0.9400	0.6458

Table 2: Annual average optical efficiency and output power table

Average optical efficiency	Average cosine efficiency	Average shadow masking efficiency	Average truncation efficiency	Average annual thermal power output (MW)	Average annual power output per unit area (kW/m^2)
0.7060	0.8584	0.9854	0.9400	42.7605	0.6803

3. Optimized design of heliostat field based on particle swarm algorithm

3.1 Particle swarm algorithm

Considering the practical application, the coordinates of the heat absorption tower should be located at or near the center of the heliostat field, so the initial coordinates of the collector center are used. To fully utilize the area, the initial layout is based on the unobstructed (EB) layout strategy. Taking the annual average thermal power output per unit mirror area as the objective, combined with the defined range and rated power constraints, the optimization model is constructed in this paper. The optimal parameters are determined by solving through particle swarm algorithm[4, 5].

Particle swarm algorithm is an optimization algorithm based on swarm intelligence, which simulates the behavior of a flock of birds foraging for food and moves the whole flock towards the optimal solution by exchanging information between individuals. The particle swarm optimization algorithm starts with a set of randomly initialized particles, each with a specific position and velocity. The algorithm first calculates the fitness of each particle and records the historical and global optimal position for it separately. In the update phase, the velocity and position of each particle are adjusted according to its best historical, global best and current position, considering some coefficients such as inertia weights and learning factors. This updating process incorporates both the particle's self-awareness and knowledge of the population's best-case scenario. The algorithm repeats this process until a predetermined number of iterations is reached or a certain convergence condition is satisfied.

3.2 Model solution

1) Define the objective function.

The objective function of the optimization decision model for the layout of the fixed-sun mirror field, i.e., the average annual output thermal power per unit mirror area. The objective function is as follows:

$$f = \frac{DNI \cdot \sum_i^N \eta_i}{N} \tag{19}$$

2) Define optimization variables.

The constraints on the size of the heliostat, the mounting height, and the value of the number of heliostats can be given by the question. At this point the optimization variables can be represented by the vectors $e = [l, w, h, N]$.

Parameterization of the particle swarm algorithm

- Number of particles generally taken as 20 -40, in this paper we take min {100, 10nvars}, *nvars* is the number of optimization parameters studied.
- Inertia weight: generally taken as 0.9, which can be fixed or change with the number of iterations. In this paper, the inertia weight is set to adaptively adjust in the range of 0.1-1.1 during the iteration process.
- Acceleration factor: generally taken as 2, it represents the weight of the particle advancing toward its own optimal position and the global optimal position.
- Maximum Speed: Generally taken as a percentage of the range of values of the optimization variable, used to limit the range of particle movement.
- Termination condition: set a reasonable maximum number of iterations, this paper takes $200nvars$.

3) Initialize the particle swarm.

A set of solutions satisfying the constraints are randomly generated as the initial positions and velocities of the particles, and the optimal solution is found following the steps in the previous section.

Based on the initial heliostat field layout setup, optimal solutions regarding heliostat dimensions, mounting height and number of heliostats are derived in this paper. Further, the positional coordinates of the absorption tower and the position of the heliostats are again considered as optimization variables and solved by particle swarm algorithm. The objective function is defined as the average annual thermal power output per unit mirror area. In this model, the position of the heliostat is bounded by the EB layout, while the constraints on the position of the absorption tower have been specified in the previous formulation. Using the same parameters of the particle swarm algorithm as before and following the defined steps, the optimal solution can be solved. Therefore, the optimization results of this paper are shown in Tables 3 to Tables 5 follows:

Table 3: Average optical efficiency and output power on the 21st day of each month

Data	Average optical efficiency	Average cosine efficiency	Average shadow masking efficiency	Average truncation efficiency	Average annual power output per unit area (kW/m^2)
January 21	0.7138	0.8857	0.9739	0.9400	0.7298
February 21st	0.7508	0.9317	0.9791	0.9400	1.2839
March 21st	0.7675	0.9524	0.9828	0.9400	1.0673
April 21st	0.7732	0.9595	0.9816	0.9400	1.0201
May 21st	0.7688	0.9539	0.9919	0.9400	1.6670
June 21st	0.7512	0.9322	0.9878	0.9400	1.3586
July 21st	0.7161	0.8886	0.9755	0.9400	0.7493
August 21st	0.6568	0.8150	0.9900	0.9400	1.0156
September 21st	0.5846	0.7254	0.9907	0.9400	0.7877
October 21st	0.5474	0.6793	0.9773	0.9400	0.6924
November 21st	0.5836	0.7241	0.9947	0.9400	0.7840
December 21st	0.6534	0.8108	0.9943	0.9400	1.3468

Table 4: Annual average optical efficiency and output power table

Average optical efficiency	Average cosine efficiency	Average shadow masking efficiency	Average truncation efficiency	Average annual thermal power output (MW)	Average annual power output per unit area (kW/m^2)
0.6889	0.8549	0.9850	0.9400	62.1795	1.2085

Table 5: Optimized design of heliostat field

Absorption tower position coordinates	Size of Fixed Sun Mirror (W×H)	Installation height of heliostat (m)	Total number of heliostats	Total area of heliostat (m^2)
(0, 0)	7×7	4	1050	51450

4. Conclusions

In the field of heliostat mirror field design, the selection of parameters is particularly critical. In this paper, it is pointed out that by precisely adjusting the mirror height, mirror width and its mounting height, not only can the output power of the heliostat mirror field be significantly adjusted, but also ensure that the annual average output thermal power per unit mirror area is maximized. In addition, the optical efficiency calculation model developed in this paper performs well in considering the shadow loss of the heliostat mirror field, providing a comprehensive and detailed calculation method. In particular, the model can consider the light scattering effect between heliostats due to their height and mounting position. However, it should be noted that to simplify the calculation, fixed values are used in this study for the collector truncation efficiency, which may lead to some bias. To further improve the accuracy and application value of the model, subsequent studies should carry out a more in-depth analysis of this efficiency, and combine it with the actual application requirements, environmental factors, and technical limitations to carry out meticulous parameter optimization, thus promoting the design and application of heliostat fields to a higher level.

References

[1] Sun H. Research and optimization of fixed-sun mirror field layout based on mixed-strategy whale optimization algorithm[D]. Lanzhou Jiaotong University, 2022. DOI: 10. 27205/d. cnki. gltec. 2022. 000117.

[2] Sun Hao, Gao Bo, Liu Jianxing. Research on the layout of fixed-sun mirror field of tower solar power plant[J]. Power Generation Technology, 2021, 42(06):690-698.

[3] Noone C J , Torrilhon M , Mitsos A .Heliostat field optimization: A new computationally efficient model and biomimetic layout[J].Solar Energy, 2012, 86(2):792-803.DOI:10.1016/j.solener.2011.12.007.

[4] Gao Weidong. Optimization study of fixed-sun mirror field scheduling for tower solar power plant [D]. North China Electric Power University, 2021. DOI: 10. 27139/d. cnki. ghbdu. 2021. 000683.

[5] Cheng S. L. Research on optimal design of tower power plant mirror field layout based on optical efficiency [D]. Hefei University of Technology, 2018.